

An Explicit/Multi-Parametric Controller Design for Pressure Swing Adsorption System

Harish Khajuria*, Efstratios N. Pistikopoulos**

*Centre for Process System Engineering, Imperial College,
London, SW7 2AZ, UK, (email: h.khajuria07@imperial.ac.uk)

**Centre for Process System Engineering, Imperial College,
London, SW7 2AZ, UK, email: (e.pistikopoulos@imperial.ac.uk)

Abstract: Pressure swing adsorption (PSA) is a flexible, albeit complex gas separation system. Due to its inherent nonlinear nature and discontinuous operation, the design of a model based PSA controller especially with varying operating conditions, is a challenging task. This work focuses on the design of an explicit/multi-parametric model predictive controller for a PSA system. Based on a system involving four adsorbent beds separating 70 % H₂, 30 % CH₄ mixture into high purity hydrogen, the key controller objective is to fast track H₂ purity to the set point value of 99.99 %. To perform this task, a rigorous and systematic framework is employed. First, a high fidelity PDAE based model is built to mimic the real operation and understand its dynamic behavior. The same model is also used to derive a linear approximate model by applying suitable system identification techniques. Then a model predictive control step is formulated for the reduced model where latest developments in multi-parametric programming are applied to derive a suitable explicit MPC controller. To test the performance of the designed controller and further refine the tuning parameters, closed loop simulations are performed where the PDAE model developed in earlier step act as virtual plant. Comparisons studies of the derived explicit MPC controller are also performed with conventional PID controllers.

Keywords: PSA, multi-parametric MPC, advanced control, system identification, PDAE based models

1. INTRODUCTION

PSA is one of the unit operations where invention occurred before the underlying theories behind it were fully understood. The Skarstrom cycle (Ruthven, 1994), one of the primitive PSA cycle, was invented in 1959 and involved only two adsorbent beds for separating air into pure oxygen or nitrogen. Since then the PSA technology has evidenced substantial growth in terms of size, complexity and versatility. A modern PSA plant can have more than 16 beds, interconnected through 100s of switch valves whose active states keep changing with time, making the real operation difficult to model and control. Studies on PSA control are quite scarce even though there is an ever increasing demand to improve the control methodology (Vinson, 2006). Model based predictive control (MPC) seems to be an appropriate control methodology for these highly complex, interconnected dynamic systems, which is the subject of this work.

2. EXPLICIT/MULTI-PARAMETRIC PROGRAMMING FRAMEWORK FOR CONTROLLER DESIGN

Fig. 1 outlines the systematic, rigorous and scientific framework pursued to perform this task. It starts with designing rigorous, first principle based, nonlinear dynamic (PDAE) model of the PSA system. In the next step, system identification techniques are used to derive a linear state

space model from the nonlinear PDAE system model. Random pulses and step change signals are used to perturb the PDAE model for this purpose. Next, multi-parametric programming algorithms are employed along with the reduced model evaluated in the previous step to design the explicit/multi-parametric controller. As a final step, closed loop simulations are conducted to rigorously test the performance of the designed controller.

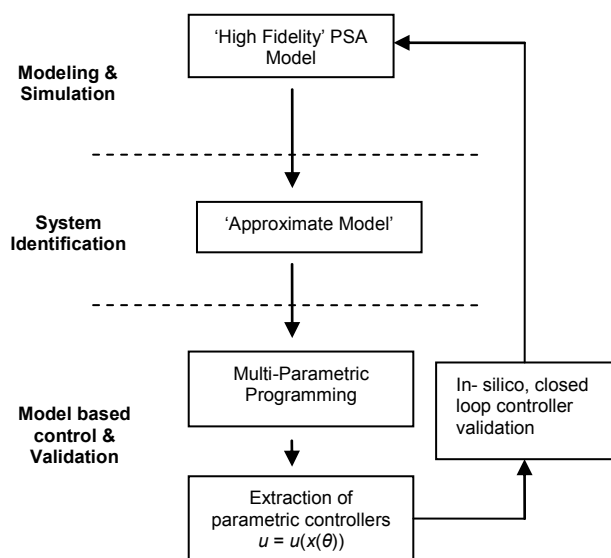


Fig. 1. A framework for designing explicit/multi-parametric MPC

Table 1: Overview of literature studies on PSA dynamic modeling (Z = Zeolite, AC = Activated carbon)

| Authors | Feed Mixture | PSA Cycle | Adsorbent/Isot herm | Mass Transfer | Heat Effects | Pressure Effects | Dispersive effects | Valve modelling |
|-----------------------------------|--|------------------------|---|---|---|--|-----------------------------|-----------------|
| Yang and Doong (1985) | H ₂ /CH ₄ , H ₂ bulk separation | 1 bed, 5 steps | AC, Langmuir-Freundlich | Pore diffusion model | Non isothermal | No gradients | Ideal plug flow | No |
| Farooq, et al. (1989) | Air, O ₂ production | Skarstrom cycle | Z, Langmuir | LDF (Linear driving force model) | Isothermal | No gradients, stays constant during adsorption & purge | Axially dispersed plug flow | No |
| Rota and Wankat (1990) | | | | Various limiting cases of internal and external resistances | Non isothermal | Blake-Kozeny equation | Ideal plug flow | No |
| Kumar (1994)/Kumar, et al. (1994) | H ₂ /CH ₄ , H ₂ purification | 4 beds, 9steps | Langmuir | LDF | Non isothermal | Ergun's equation | Ideal plug flow | Yes |
| Warmuziński and Tańczyk (1997) | H ₂ from coke gas | PSA in series, 8 steps | Loading ratio Correlation | LDF | Non isothermal | No gradients | Axially dispersed plug flow | No |
| Yang and Lee (1998) | H ₂ purification from coke oven gas | 2 bed, 7 steps | Layered adsorbent - Z & AC, Langmuir-Freundlich | LDF | Non isothermal | Ergun's equation | Axially dispersed plug flow | No |
| Grande and Rodrigues (2005) | Propane - propylene separation | 1 bed, 5 steps | Z, Multisite Langmuir | Both internal and external resistances considered | Non isothermal, separate equations for fluid, solid and column wall | Ergun's equation | Axially dispersed plug flow | No |
| Ribeiro, et al. (2008) | H ₂ purification from H ₂ /CH ₄ /CO/CO ₂ /N ₂ | 1 and 4 beds, 5cycle | Layered adsorbent - AC & Z, Multisite Langmuir | Both internal and external resistances considered | Non isothermal, separate equations for fluid, solid and column wall | Ergun's equation | Axially dispersed plug flow | No |

2.1. PSA Mathematical Modelling

In past, significant contributions to capture the PSA dynamic behaviour by first principle based models have been made; brief overview of which is shown in Table 1. In this work, a rigorous first principle based PDAE model of PSA is created in gPROMS. The model (Table 2) incorporates mass, momentum and energy balance equations for the gas-solid system. Adsorption dynamics is captured by multisite Langmuir adsorption isotherms. It also incorporates the axial dispersion in heat and mass transfer balances. Time varying boundary conditions, corresponding to each process step at both ends of the column are also modelled in detail to perform the PSA cyclic operation.

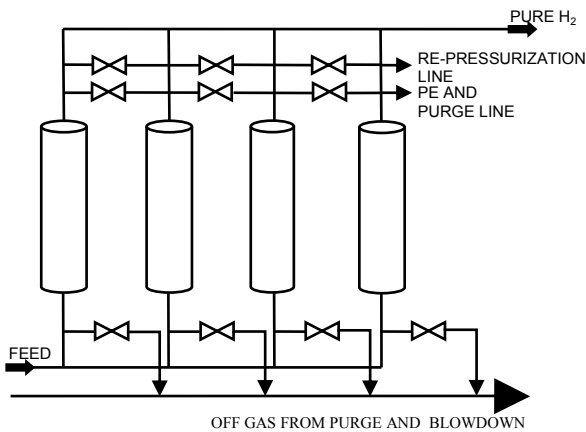


Fig. 2. Four bed, multiple switch valve PSA configuration employed in this study

Table 2. Key features of the PSA dynamic model

| |
|--|
| Individual component balance $\frac{\partial C_i}{\partial t} + \frac{\partial UC_i}{\partial Z} + \rho_p \frac{1 - \epsilon}{\epsilon} \frac{\partial \bar{Q}_i}{\partial t} = D_{Zi} \frac{\partial^2 C_i}{\partial Z^2}$ |
| Energy balance $\frac{\partial (\sum_i (C_{pi} - R) C_i) T}{\partial t} + C_{ps} \rho_p \frac{1 - \epsilon}{\epsilon} \frac{\partial T}{\partial t} + \frac{\partial (\sum_i C_{pi} C_i UT)}{\partial Z} + \rho_p \frac{1 - \epsilon}{\epsilon} \sum_i \frac{\partial \bar{Q}_i}{\partial t} \Delta H_i + \frac{4h(T - T_w)}{\epsilon D} = \lambda \frac{\partial^2 T}{\partial Z^2}$ |
| Gas phase momentum balance $-\frac{\partial P}{\partial Z} = \frac{150\mu(1 - \epsilon)^2}{\epsilon^3 d_p^2} U + \frac{1.75(1 - \epsilon) \sum C_i MW_i}{\epsilon^3 d_p} U U$ |
| Multisite Langmuir Isotherm (Ribeiro, et al., 2008) $\frac{Q_i^*}{Q_i^{max}} = a_i K_i C_i RT \left[1 - \sum_i \left(\frac{Q_i^*}{Q_i^{max}} \right) \right]^{a_i}$ $K_i = K_{\infty} \exp\left(\frac{-\Delta H_i}{RT}\right)$ |
| LDF rate expression $\frac{\partial \bar{Q}_i}{\partial t} = K_{LDFi} (Q_i^* - \bar{Q}_i)$ |
| Valve equation $U = \begin{cases} \frac{R}{\epsilon \pi D^2} \phi C_V 1.1792486 \sqrt{1 - \left(\frac{P_L}{P_H}\right)^2} & \text{if } \frac{P_H}{P_L} < P_{CRITICAL} \\ \frac{R}{\epsilon \pi D^2} \phi C_V 1.1792486 \sqrt{1 - \left(\frac{1}{P_{CRITICAL}}\right)^2} & \text{Otherwise} \end{cases}$ $P_{CRITICAL} = \left(\frac{2}{1 + \gamma}\right)^{\frac{\gamma}{1 - \gamma}}, \gamma = \frac{C_p}{C_p - R}$ |

Fig. 2 shows the four-bed PSA system considered for this particular study. Each of the four beds contains activated carbon as an adsorbent and it undergoes a cyclic operation comprising of nine process steps (Kumar (1994)), separating a 70% H₂ and 30 % CH₄ mixture into pure hydrogen. Furthermore, time duration of two process steps which can be actually varied by the user is assumed to be the same (and denoted as adsorption time in rest of the article). Appendix A provides the details of feed stream and geometrical design parameters of PSA system under study.

2.2. System Identification

Numerous open loop simulations are conducted with different types of input signals to perturb the system (PDAE), and consecutively linear models suitable for model based control purposes are extracted. Step change and random pulse signals are studied for this task where in particular, design of random pulse signals requires selection of two critical parameters; (i) selecting the maximum change to be allowed in signal amplitude from its base value. A very large change could perturb the system beyond the scope of fitting a single linear model. On the other hand, small changes do not disturb the system sufficiently to reveal its complete dynamic nature eventually, leading to poor model identification. (ii) Selecting the switching time for the pulse, i.e. the time for which the signal stays constant before *switching* to the new random value. Very high values of switching time produces input-output behavior close to a step input change.

In order to fix the first parameter, open loop experiments are performed with step signals of various step sizes, and a value of 3 seconds is finally selected. For the second parameter a well structured, closed loop simulations based approach is employed; wherein three random pulse signals are designed with the same magnitude (first parameter) but with different switching times, resulting in a library of reduced models. Furthermore, the best switching time is decided based on their closed loop performances which is discussed in the next section.

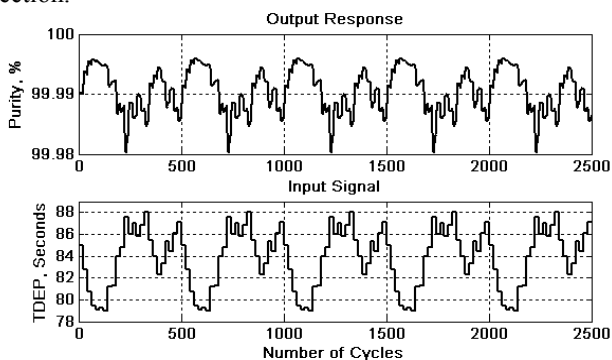


Fig. 3. Input (adsorption time, TDEP)-output (purity) response with switching time of 20 cycles

Fig. 3, for example, shows the input-output response for a signal with switching time of 20 cycles used with the MATLAB system identification toolbox. An 8th order state space model (appendix C) provides the best fit for it and is thus chosen as the prediction model for MPC purposes. Its performance comparison with the PDAE model is shown in Fig. 4, for the last 500 cycles (of Fig. 3). Similarly, switching

times of 5 cycles, 80 cycles are also studied. Moreover, conventional step input (infinite switching time) is also considered where adsorption time changes from 115 seconds to 55 seconds and only first few cycles data is considered for system identification, as purity response during this time forms an S shaped curve.

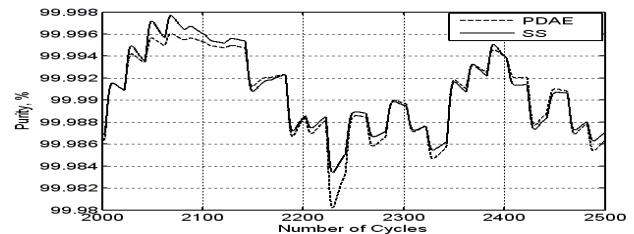


Fig. 4. Plot showing the comparison of an 8th order state space (SS) model response with the original PDAE model to the random signal used in Fig. 3.

2.3. PSA model based control and validation

The control objective, in this study is defined as fast tracking of hydrogen purity to set point of 99.99 %. Fig. 5 shows the long term variation of hydrogen purity with adsorption time obtained by performing simulations on the base case system (Appendix A).

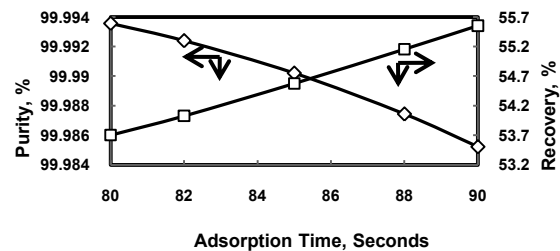


Fig. 5. Variation of PSA purity and recovery at cyclic steady state (CSS) with adsorption time

Furthermore, Fig. 6 shows the short term response of hydrogen purity when a random pulse signal of adsorption time with switching time of 20 cycles is used to perturb the system. The instant response of system purity to adsorption time changes make adsorption time a suitable choice of input variable for purity control.

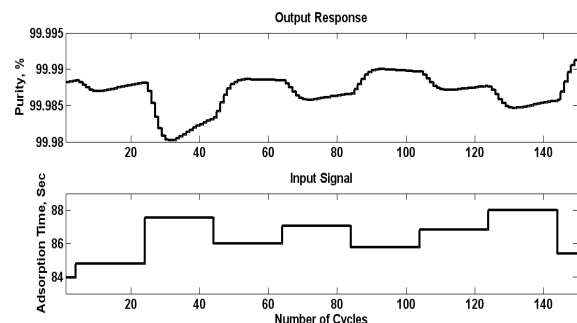


Fig. 6. Short term time response of purity to changes in adsorption time

It is also evident from Fig. 5 that changes in adsorption step duration not only affect product purity but product recovery as well. Clearly, adsorption step time should not go to very low values to avoid uneconomical (low recovery) operation.

Another important constraint on change in adsorption step time is the limited or fixed adsorbent capacity. When adsorption step duration increases or decreases, the amount of impurities entering the bed and getting adsorbed also changes accordingly. Since, a given amount of solid adsorbent can accommodate only a limited amount of impurities, a large increase in adsorption step time can saturate the bed and make it unsuitable for the future use. This means, that both high values of adsorption time and large changes in adsorption time should be avoided, while controller decides its action. A Model based controller, which incorporates the above mentioned operational constraints in its optimization framework is formulated in (1) to (4). Here, y is the control variable purity, and u is the manipulative variable, adsorption time. N and M represents the prediction and control horizon, respectively and k is a particular sampling instant. Sampling interval is taken as one complete PSA cycle. Also, N and M are fixed to values 4 and 2, respectively, and (2) is used for state estimation purposes.

$$\min_u Z = \sum_{k=1}^{N-1} (y_k - y_k^R)(y_k - y_k^R) + \sum_{k=0}^{M-1} \Delta u_k' R \Delta u_k \quad (1)$$

s.t.

$$x_{k+1} = Ax_k + bu_k \quad (2)$$

$$y_k = cx_k \quad (3)$$

$$55 \leq u_k \leq 115 \quad (4)$$

An inherent feature of MPC controller is the online solution of optimization problem ((1) to (4)), as the state of system continuously evolves in time. The repeated online optimization procedure depending on the size of problem formulated could be a computationally intensive task. Furthermore, in some cases, for a given set of state variables the optimization problem could become infeasible and as a result controller gives an incorrect value of the plant input variable. In this work, novel multi-parametric methodology proposed by Pistikopoulos, et.al. (2000) are employed to overcome these popular limitations of MPC. With the application of multi-parametric programming techniques, the original optimization problem is solved offline, providing the control law in an explicit form, beforehand (Pistikopoulos et. al., 2007a, 2007b) it is implemented online.

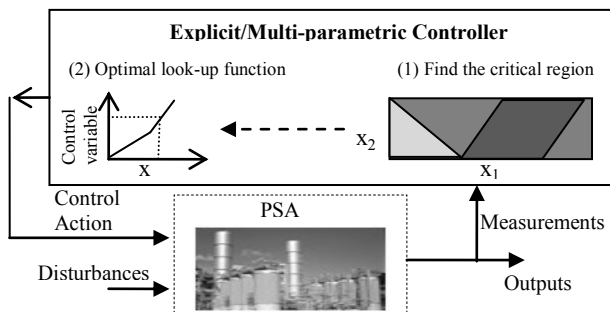


Fig. 7. Online implementation of an explicit/multi-parametric controller

During the online operation, as shown in Fig. 7, the plant measurements are provided to the explicit/multi-parametric

controller, which then searches for the critical region belonging to this particular state variable set and consecutively, extracts the corresponding control law. The computational work of evaluating the critical regions and the corresponding control laws is performed offline (apriori) and is stored for online use (later). For the reduced system represented in Appendix C (8th order SS model), the multi-parametric control framework formulates 11 parameters listed in Table 3. The table also shows the range for which each parameter is varied, where the last two variables are scaled variables with the following rule, $y^* = (y - 0.9999)100000$.

Table 3. Range of parameters used in explicit/multi-parametric controller formulation for switching time of 20 cycles experiment

| | | | | | |
|-------|------------|-------|------------|----------|------------|
| x_1 | [-100 100] | x_5 | [-100 100] | $u(k-1)$ | [55 115] |
| x_2 | [-100 100] | x_6 | [-100 100] | y^* | [-100 10] |
| x_3 | [-100 100] | x_7 | [-100 100] | y^{R*} | [-0.1 0.1] |
| x_4 | [-100 100] | x_8 | [-100 100] | | |

Next, the MPC problem in (1) to (4) is reformulated as a multi-parametric QP problem, whose offline solution leads to 7 critical regions when R is kept at a particular value of 30. The two dimensional projection of the 7 dimensional critical region polyhedral obtained by fixing all but first two parameters (Table 3) is displayed in Fig. 8.

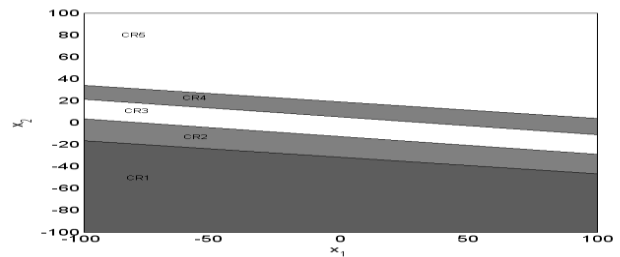


Fig. 8. Two dimensional slice of critical region (CR) polyhedral corresponding to SS model in Appendix C, $N = 4$, $M = 2$ and $R = 30$

2.3.1. Closed Loop Validation

To evaluate the performance of the designed controllers, PSA feed flow rate is step increased by 10 % from its design value and closed loop simulations are conducted with MPC tuning factor R (from (1)) varying from 0 to 180. The high fidelity PDAE model now acts as the virtual plant for performing the closed loop simulations. Fig. 9 compares the closed loop performance of a number of explicit/multi-parametric MPC controller configurations, where each line corresponds to the reduced models derived in the system identification step. Also, in these plots, to better understand and quantify the closed loop behaviour all closed loop simulation results have been concentrated in terms of two performance indicators.

The first PSA control performance indicator, the controller response time is defined as the minimum number of PSA cycles required to permanently overcome the disturbance and bring the purity back to its set point of 99.99 %. The second performance indicator is the mean control effort (Δu) made

by the controller during the response time (first performance indicator). Maximum value of Δu during the response time is also measured. Large value of this performance indicator highlights any violation of operational constraints on adsorption time changes mentioned earlier.

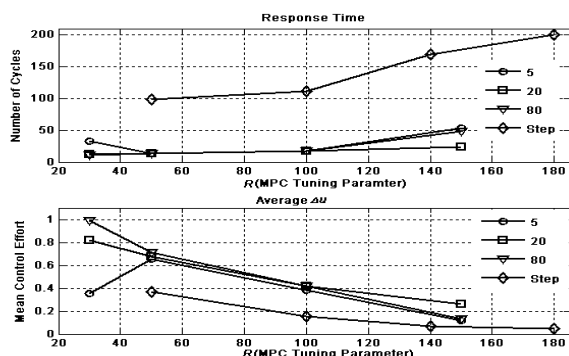


Fig. 9. Closed loop performance comparison for various reduced models against two key PSA performance indicators

From the plots, it is evident that increasing R slows down the controller response time while it decreases the mean control effort. This behaviour can be attributed to the particular type of objective function used in (1). It can also be observed that controller configurations built from random signals generated reduced models, provides better close loop performance than a simple step test generated reduced model. In particular, controller configuration designed from the reduced model with switching time of 20 cycles gives the best performance, as it (Appendix C) not only gives the least value of first performance indicator for a wide range of R but also keeps the second performance indicator under check. Furthermore, the best R value for this controller seems to be 30 as it provides the least value of the first performance indicator. Henceforth, this is the controller setting used for comparing explicit/multi-parametric MPC with conventional PID controller.

2.3.2. Comparison with PID Controller

To further assess and compare the strength of model based explicit/multi-parametric MPC controller with the conventional controllers, a PID controller is also designed. The systematic design procedure is as follows; (1) the autotuning method of Åström and Hägglund (Seborg, et al., 1989) is used to evaluate the ultimate gain and ultimate period of the purity-adsorption time loop. (2) Next, these values are in turn used to derive the initial guess of PID tuning parameters namely, proportional gain, integral time and derivative time using the Z-N tuning relations. (3) These tuning parameters are further refined, till the best results in terms of the two PSA controller performance indicators, are obtained. The comparison results displayed in the first part of Table 4, highlights that model based controller is twice as fast the PID controller, which is a considerable improvement in terms of speed of response. The same results also show that it achieves this task by maintaining the control effort at lower values. To further evaluate the strength of explicit/multi-parametric controller, the PSA system is perturbed with an impulse disturbance. During the simulations, the MPC and

PID tuning parameters are retained at their respective best values as evaluated in the step disturbance study.

Table 4. Multi-parametric MPC –PID comparison

| 10 % step increase in PSA feed | | | |
|-----------------------------------|------------------------|------------------------------|------------------------------|
| Controller | Response Time (Cycles) | Average Δu (Seconds) | Maximum Δu (Seconds) |
| MPC | 13 | 0.6748 | 1.4090 |
| PID | 25 | 0.8367 | 5.1183 |
| 35 % impulse increase in PSA feed | | | |
| MPC | 7 | 0.6619 | 1.5787 |
| PID | 5 | 4.7156 | 12.1161 |
| Open Loop | 9 | | |

The comparisons of PSA controller performance indicators for both types of controllers are shown in Table 4. The disturbance this time is so fast that the open loop response settles down in nine PSA cycles. As a result, response time of PID and explicit MPC is almost same but the second PSA performance indicator for PID comes out to be much larger than the MPC. PID result shows that during the response time maximum Δu is around 12 seconds. This is a large number and such a big change in adsorption time, as discussed earlier, can cause damage to the solid adsorbent. The model based control, on the other hand, provides a much better and safer response to the disturbance as shown in Fig. 10.

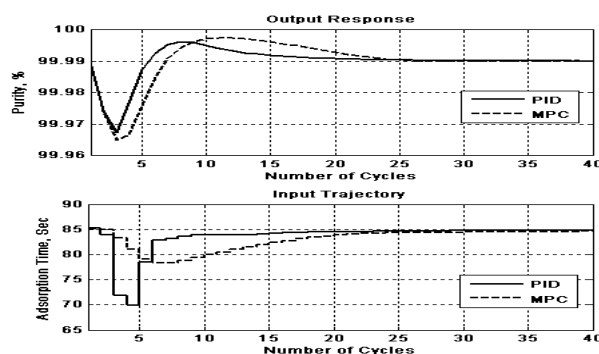


Fig. 10. Closed loop comparison of MPC and PID controllers for impulse disturbance of 35 % in PSA feed

3. CONCLUSIONS AND FUTURE WORK

An explicit MPC controller is designed for a PSA system employing a systematic multi-parametric framework approach. The designed explicit MPC is also compared in detail with the current state of art PID controllers. In future studies, the effect of recovery-adsorption time dynamics will also be incorporated in the system identification process, making it more challenging but also explicitly incorporating the purity-recovery tradeoff in model based control framework. Ultimately, the controller design will be made robust to obtain better performance in presence of the operational noises.

ACKNOWLEDGEMENTS

Financial support from the Royal Commission for the Exhibition of 1851, ParOS Ltd., EU project HY2SEPS, and KAUST is sincerely acknowledged.

REFERENCES

- Farooq, S., Ruthven, D. M. & Boniface, H. A. (1989), Numerical simulation of a pressure swing adsorption oxygen unit, *Chemical Engineering Science* **44**(12), 2809 – 2816.
- Grande, C. A. & Rodrigues, A. E. (2005), Propane/Propylene Separation by Pressure Swing Adsorption Using Zeolite 4A, *Ind. Eng. Chem. Res* **44**, 8815–8829.
- Kumar, R. (1994), Pressure Swing Adsorption Process: Performance Optimum and Adsorbent Selection, *Industrial & Engineering Chemistry Research* **33**(6), 1600-1605.
- Kumar, R., Fox, V. G., Hartzog, D. G., Larson, R. E., Chen, Y. C., Houghton, P. A. & Naheiri, T. (1994), A versatile process simulator for adsorptive separations, *Chemical Engineering Science* **49**(18), 3115 - 3125.
- Pistikopoulos, E. N.; Dua, V.; Bozinis, N. A.; Bemporad, A. & Morari, M. (2000), On-line optimization via off-line parametric optimization tools, *Computers & Chemical Engineering* **24**(2-7), 188 - 188.
- Pistikopoulos, E.N., Georgiadis, M. & Dua, V. (2007a), *Multi-parametric Programming: Theory, Algorithms and Applications*, Weinheim: Wiley-VCH.
- Pistikopoulos, E.N., Georgiadis, M. & Dua, V. (2007b), *Multi-parametric Model-based Control: Theory and Applications*, Weinheim: Wiley-VCH.
- Ribeiro, A. M., Grande, C. A.; Lopes, F. V.; Loureiro, J. M. & Rodrigues, A. E. (2008), A parametric study of layered bed PSA for hydrogen purification, *Chemical Engineering Science* **63**(21), 5258 - 5273.
- Rota, R. & Wankat, P. C. (1990), Intensification of pressure swing adsorption processes, *AIChE* **36**(9), 1299-1312.
- Ruthven, D. M.; Farooq, S. & Knaebel, K. S. (1994), *Pressure Swing Adsorption*, Wiley-VCH
- Seborg, D. E., Edgar, T. F. & Mellichamp, D. A. (1989), *Process Dynamics and Control*, John Wiley & Sons.
- Vinson, D. R. (2006), Air separation control technology, *Computers & Chemical Engineering* **30**(10-12), 1436 - 1446.
- Warmuzinski, K. & Tanczyk, M. (1997), Multicomponent pressure swing adsorption Part I. Modelling of large-scale PSA installations, *Chemical Engineering and Processing* **36**(2), 89 - 99.
- Yang, J. & Lee, C.-H. (1998), Adsorption dynamics of a layered bed PSA for H₂ recovery from coke oven gas, *AIChE* **44**(6), 1325-1334.
- Yang, R. T. & Doong, S. J. (1985), Gas Separation by Pressure Swing Adsorption: A Pore-Diffusion Model for Bulk Separation, *AIChE Journal* **31**(11), 1829-1842.

Appendix A. Base case - PSA System

| | | | |
|-------------------------|-----|----------------------|--------|
| Feed pressure (bars) | 7 | Bed length (m) | 0.445 |
| Blowdown pressure (atm) | 1 | Bed diameter (m) | 0.072 |
| Bed Porosity | 0.4 | Feed temperature (K) | 303.15 |
| Feed flow rate (SLPM) | 8.5 | No. of axial grids | 40 |

Appendix B. Partial nomenclature for the dynamic model in Table 2

| | | |
|---------------|---|--------------------|
| C_i | Gas phase molar concentration of species i | mol/m ³ |
| C_V | Valve constant | |
| C_{P_i} | Gas phase molar specific heat at constant pressure | J/mol K |
| C_{P_s} | Solid phase mass specific heat at constant pressure | J/Kg K |
| D | Bed diameter | M |
| D_{Z_i} | Axial mass dispersion coefficient for the species i | m ² /s |
| h | Convective heat transfer coefficient between fluid and wall | W/m ² K |
| K_{LDF_i} | LDF rate constant | 1/s |
| L | Bed length | M |
| P | Bed pressure | Pa |
| Q_i^* | Adsorbed phase concentration in equilibrium with bulk gas for species i | mol/Kg |
| \bar{Q}_i | Volume averaged adsorbed phase concentration of species i | mol/Kg |
| Q_i^{max} | Maximum adsorbed phase concentration in equilibrium with bulk gas for species i | mol/Kg |
| R | Ideal gas constant (8.314) | J/mol K |
| t | Time | S |
| T | Gas or solid phase temperature | K |
| T_W | Wall temperature | K |
| U | Fluid interstitial velocity | m/s |
| Z | Axial position | M |
| ε | Bed porosity | |
| λ | Axial heat transfer coefficient | W/m K |
| ϕ | Dimensionless constant | |

Appendix C. Best fit state space model matrices for input-output response in Fig. 3.

$$A = \begin{bmatrix} 0.995 & -0.095 & -0.001 & 0.000 & 0.001 & -0.001 & 0.001 & 0.000 \\ 0.074 & 0.901 & 0.327 & 0.068 & 0.073 & 0.003 & -0.010 & -0.003 \\ -0.063 & -0.329 & 0.536 & -0.289 & -0.300 & -0.085 & 0.032 & 0.089 \\ 0.002 & -0.024 & 0.121 & 0.763 & -0.658 & 0.208 & 0.100 & -0.038 \\ 0.009 & -0.029 & 0.358 & -0.240 & 0.089 & 0.400 & -0.040 & 0.011 \\ 0.000 & -0.004 & 0.054 & -0.014 & -0.083 & -0.793 & -0.623 & 0.289 \\ -0.002 & 0.001 & -0.028 & -0.052 & -0.075 & 0.455 & -0.604 & 0.668 \\ -0.001 & 0.001 & 0.016 & 0.049 & 0.090 & -0.191 & -0.375 & 0.051 \end{bmatrix}$$

$$b' = \begin{bmatrix} -0.009 & 0.0145 & -0.0266 & 0.0207 & 0.041 & 0.0095 & 0.0208 & 0.0907 \end{bmatrix}$$

$$c = \begin{bmatrix} 182.14 & -8.4 & -0.827 & -0.189 & -0.148 & -0.052 & 0.089 & 0.034 \end{bmatrix}$$